

Wetting transitions of hydrogen and deuterium on the surface of alkali metals

Wei Shi and J. Karl Johnson*

*Department of Chemical and Petroleum Engineering, University of Pittsburgh, Pittsburgh, Pennsylvania 15261, USA
and National Energy Technology Laboratory, Pittsburgh, Pennsylvania 15236, USA*

M. W. Cole

Department of Physics and Materials Research Institute, Pennsylvania State University, University Park, Pennsylvania 16802, USA

(Received 12 May 2003; published 2 September 2003)

Although wetting transitions have been observed for helium and hydrogen on alkali metal surfaces, no finite temperature, quantum simulation studies of these systems have been able to conclusively locate a wetting transition. This paper presents such calculations for the systems H_2 and D_2 on Rb and Cs, using semiempirical hydrogen-hydrogen interactions and *ab initio* gas-surface interactions. Comparison with experiment implies that the adsorption potential is $\sim 10\%$ more attractive than is predicted by current theory. Simulations of H_2 adsorbing on a 15 Å thick film of Rb on Au predict that this system will show a decrease in the wetting temperature of about 1 K compared with H_2 on pure Rb. The simulations reveal that a commonly used “simple model” is surprisingly accurate.

DOI: 10.1103/PhysRevB.68.125401

PACS number(s): 68.08.Bc, 05.30.-d, 67.70.+n, 82.60.-s

I. INTRODUCTION

Consider a fluid near a solid surface at pressure P and temperature T (below the liquid-vapor critical temperature T_c). When P is equal to the saturated vapor pressure (P_{SVP}), an adsorbed liquid film may exhibit either one of two possible behaviors: spreading across the surface or beading up to form a droplet. These possibilities are called wetting (or complete wetting) and nonwetting (or incomplete wetting), respectively. This distinction is compatible with Young's equation for the contact angle (which vanishes in the wetting case) and thus the behavior of a given system can, in principle, be derived from the T dependence of three surface tensions (gas-solid, liquid-solid, and gas-liquid). Some 25 years ago, scenarios of thermodynamic transitions between wetting and nonwetting were predicted by Cahn¹ and Ebner and Saam.² Subsequently, such wetting transitions have been observed experimentally for both isotopes of He^{3-8} (the $^3He/Cs$ case involves a prewetting transition at low temperature, but the film does wet the surface at all T) and for hydrogen⁹⁻¹¹ on Rb and Cs, for Ne on Rb,¹² and for Hg on sapphire and Ta.^{13,14} Similar transitions have been predicted to occur for other adsorption systems (e.g., Ne/Mg and Ar, Kr, and Xe on alkali metal surfaces).¹⁵⁻¹⁷ The common feature of all of these systems is the existence of a very weakly attractive adsorption potential; the well depth (D) of the gas-surface interaction $V(z)$ is less than, or of the order of, the well depth (ϵ) of the intermolecular potential of the adsorbing fluid.

These wetting transitions have been studied by a variety of general theoretical models, including lattice-gas, density functionals, and classical Monte Carlo simulations.¹⁸⁻²³ To date, remarkably, there has been no finite temperature quantum simulation definitively exhibiting a wetting transition, even though the quantum fluids He and H_2 are paradigms of this transition.²⁴ To our knowledge, only three simulation studies of wetting transitions have been published for quantum fluids.²⁵⁻²⁷ All of these studies have utilized the path

integral formalism²⁸ to account for the quantum mechanical properties of the fluids. However, none of the simulations has resulted in conclusive demonstration of the existence of a wetting transition or a direct observation of a prewetting transition. Wagner and Ceperley were the first to employ path integral methods to search for a wetting transition. They studied 4He adsorbed on a H_2 substrate at a temperature of 0.5 K. This system was predicted to exhibit a wetting transition by Cheng *et al.*²¹ Wagner and Ceperley computed the binding energy of 4He on three different models of an H_2 surface and found a slight minimum in the binding energy with respect to coverage. While a minimum in the binding energy is a signature of a wetting transition at zero temperature, these calculations were performed at finite temperature, where the situation is less clear. Their calculations were carried out on very small systems, for which finite size effects can change the appearance of a wetting transition. Therefore, that study was not a definitive observation of a wetting transition for a quantum fluid at finite temperature.

Boninsegni and Cole studied 4He on a Cs surface using a fixed volume and a fixed number of He atoms.²⁶ This system was also limited in size, containing only 64 atoms on a smooth Cs surface. The authors point out that the results from such a small system are only qualitatively representative of the true system.²⁶ They observe that the 64 4He atoms tend to form something like a droplet at a temperature of 0.67 K and tend to be close to wetting the surface at 2 K. Thus, they do not claim to have observed a wetting transition and only conclude that their simulations are “qualitatively consistent” with a wetting transition occurring in the vicinity of 2 K.

Bojan *et al.* used the same methods we use here to search for a wetting transition for H_2 on Rb.²⁵ However, the lengths of the simulation runs were too short to provide definitive results. In addition, no precise values of the bulk vapor-liquid saturation chemical potential from simulations were available at the time, making it difficult to locate a prewetting transition. They observed evidence of incomplete wet-

ting at 22 K and apparently complete wetting at 30 K, but were unable to observe a prewetting transition.

In related work Boninsegni *et al.* studied ^4He on Li using both path integral and density functional methods. The aim was to investigate superfluidity in thin He films. The $^4\text{He}/\text{Li}$ system exhibits complete wetting at all temperatures; hence, no wetting transition was observed.

The only classical simulation study pertinent to *any* experimentally observed wetting transition (Ne/Rb) is difficult to compare with experimental data because of uncertainties arising from the proximity (within 1%) of the wetting transition temperature T_w to the bulk vapor-liquid critical temperature T_c (Refs. 12,20) and neglect of quantum effects in the simulations. It is known that quantum effects are important in liquid Ne, even near the critical point.²⁹

This lack of theoretical analysis for systems studied in the laboratory leaves open many questions, e.g., how reliable are the adsorption potentials and theoretical models used to predict the transition? What is the detailed nature of the thin-to-thick film wetting transition? Can simulations accurately predict other systems which will exhibit prewetting transitions?

In the absence of exact calculations for experimentally relevant systems, an alternative approach to predicting T_w has been posited, a so-called “simple model.”²¹ In that model, the thin-to-thick film transition is predicted to occur when the surface tension “price” of forming two interfaces becomes equal to the free energy reduction due to the integrated fluid-surface attraction. Estimates of these terms lead to an implicit relation for the wetting temperature

$$\sigma_{lg} = -\frac{1}{2}\rho_0 \int_{z_{\min}}^{\infty} V(z) dz, \quad (1)$$

where σ_{lg} is the bulk liquid-vapor surface tension and ρ_0 is the bulk fluid number density, both at T_w , and the integral extends from the minimum of the potential to infinity. Some evidence implies that this model works surprisingly well in predicting T_w of classical gases, except in cases of the very least attractive interactions.²² However, no comparison between “exact” calculations, this model, and experimental data has ever been made. Such calculations are therefore needed in order to further test this model and theoretical calculations of the adsorption potential. This paper presents evidence relevant to these open questions by comparing wetting transition data with results of path integral grand canonical Monte Carlo simulations for the hydrogen isotopes. This simulation method is exact, in principle, assuming that the interaction potentials are correct.

II. COMPUTATIONAL METHODS

We have employed the real space implementation of the path integral formalism developed by Feynman²⁸ to simulate quantum fluids. In this formalism, each quantum molecule is replaced by a classical ring polymer with a number of beads. The equilibrium properties of the corresponding quantum fluid are given by the proper statistical mechanical averages over the ring polymers. The number of beads must be large enough so that the properties of the fluid do not depend on

the number of beads. In this work we found that 40 (20) beads were sufficient for modeling H_2 (D_2) at the temperatures and densities encountered in this work. We refer the reader to a recently published review of the path integral method as applied to condensed helium³⁰ for details. The path integral grand canonical Monte Carlo method³¹ was used to generate adsorption isotherms in this work. The grand canonical simulation method involves three distinct types of moves of the molecules, namely, displacements, creations, and deletions. Molecular displacements were generated using the hybrid Monte Carlo (HMC) method³² wherein all the molecules were moved in a single configurational step. The HMC method has been shown to be efficient for canonical ensemble path integral simulations.³³ The type of move to attempt was selected randomly with probability 0.01, 0.495, and 0.495 for displacements, creations, and deletions, respectively. The low probability of making a displacement was chosen because each HMC displacement consists of five MD time steps in the microcanonical ensemble. Hence, very few HMC moves are needed to propagate the system. We used the multiple time-scale reversible reference system propagator algorithm of Tuckerman *et al.*³⁴ to separate the stiff intramolecular harmonic forces (bead-bead interactions) from the more slowly varying intermolecular forces. Ten short time steps were employed for every long time step. The velocity Verlet algorithm³⁵ was used to integrate the equations of motion. Most simulation runs included 5×10^5 configurations for equilibration followed by 6×10^6 configurations for data taking.

The fluid interactions were modeled with the Silver-Goldman potential.³⁶ This potential has been shown to be accurate for producing the vapor-liquid phase diagram for both H_2 and D_2 .^{29,31,37} The pure fluid surface tension properties for liquid H_2 and D_2 computed from the Silver-Goldman potential have recently been shown to be in excellent agreement with experimentally measured surface tension over a range of temperatures.³⁸ The saturation properties of the bulk fluids were computed from multiple histogram reweighting (MHR) (Refs. 39,40) adapted for path integral Hamiltonians.³⁷ The MHR simulations provide very accurate values of P_{SVP} , which are important for studying wetting transitions.

A number of different potentials for H_2/Rb were considered, four of which appear in Fig. 1. The *ab initio* potential of Chizmeshya *et al.* (CCZ)¹⁶ was derived from a Hartree-Fock repulsion and a damped van der Waals (VDW) dispersion term.⁴¹ The resulting potential was found to fit the following expression:

$$V(z) = V_0(1 + \alpha z)e^{-\alpha z} - f_2[\beta(z)(z - z_{\text{VDW}})] \frac{C_{\text{VDW}}}{(z - z_{\text{VDW}})^3}, \quad (2)$$

where z is the distance between the adsorbate and the jellium boundary of the metal, f_2 is a damping function given by $f_2(x) = 1 - e^{-x}(1 + x + x^2/2)$, $\beta(z)$ is given as $\beta(z) = \alpha^2 z / (1 + \alpha z)$, V_0 , α , C_{VDW} , and z_{VDW} are the four parameters of the potential. The CCZ parameters for H_2 and D_2 on Rb are $V_0 = 0.274$ eV, $\alpha = 1.769 \text{ \AA}^{-1}$, $C_{\text{VDW}} = 0.297 \text{ eV \AA}^3$, and $z_{\text{VDW}} = 0.246 \text{ \AA}$. This potential is characterized by a well-depth ratio $D/\epsilon \sim 1.26$. We have also

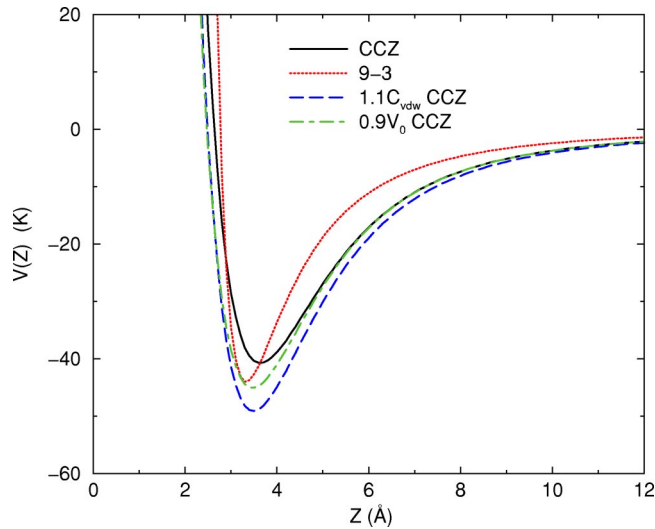


FIG. 1. (Color online) The original CCZ (Ref. 16) and the 9-3 potentials (Ref. 10) for H_2 on Rb. Also shown are two modified potentials obtained by varying the C_{vdw} and V_0 parameters in the CCZ potential.

used an empirical 9-3 potential, which was used by Cheng *et al.*¹⁰ to compute the wetting temperature for H_2 on Rb from the simple model.

For most of the simulations the simulation cell was a rectangle, 30 \AA on a side in the x and y directions, with a height (z) of 60 \AA . Periodic boundary conditions were applied in the x and y directions, with the lower xy plane being the metal surface and the upper plane a reflecting wall. Calculations done with the 9-3 potential used a cubic simulation cell 30 \AA on a side. Comparison of results for the CCZ potential for the larger and smaller cell sizes show that differences in the location of the wetting temperatures and the values of the prewetting pressures are about the same as the uncertainties in the calculations.

III. RESULTS

A signature of a prewetting transition that is observable in a simulation is the abrupt (first order) change in the amount of fluid adsorbed on a surface at constant temperature as the pressure (chemical potential) is increased toward the bulk saturation pressure. This can be observed by plotting the film density profiles over a range of pressures. This method has been used in a variety of classical simulation studies.^{18,23,42–45} Figure 2 presents simulation results for the film density, obtained with the CCZ potential, at 25 and 26 K. At 25 K, only a thin film forms for all $P < P_{SVP}$, indicating nonwetting. Note that due to metastability the adsorption is very small even at a pressure a little higher than P_{SVP} . The thermodynamic excess coverage (the integrated excess of the film density relative to the vapor density) is minuscule, about $\sim 15\%$ of the close-packed monolayer coverage. The simulation results for the film at 26 K manifest quite different behavior, characteristic of a prewetting transition. Below 98% of P_{SVP} , a thin film forms. At $P/P_{SVP} = 0.98$, however, there is a factor of 8 jump in the excess coverage. Further increases in P toward P_{SVP} yield an ever thickening film, i.e., wetting behavior. Thus, the CCZ potential yields a first order wetting transition, with a wetting temperature somewhere between these two values of T , i.e., $T_w = 25.5 \pm 0.5 \text{ K}$. The data plotted in Fig. 2 gives the first convincing evidence of a prewetting transition for a strongly quantum fluid observed from a molecular simulation. These data indicate that the prewetting pressure at 26 K for the H_2 /Rb CCZ potential occurs somewhere between $P/P_{SVP} = 0.968$ and 0.986 . From Fig. 3 we observe oscillations between the thin and thick film states at $P/P_{SVP} = 0.980$ at 26 K. Figure 3(a) shows two density profiles computed at the same relative pressure, but using different “slices” of the simulation. This can be seen from the evolution of the total number of H_2 molecules in the simulation cell as a function of time shown in Fig. 3(b). Most of the simulation explores phase space corresponding to a

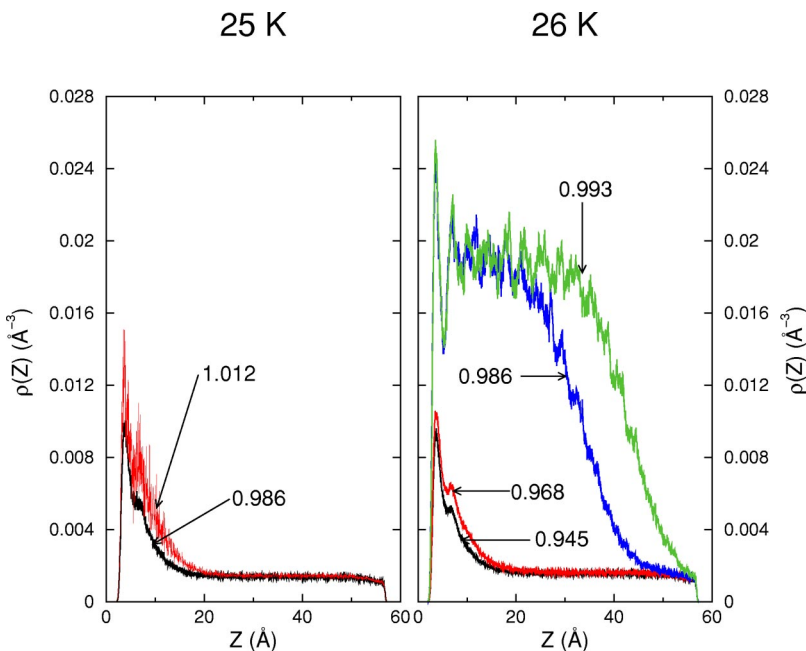


FIG. 2. (Color online) The local density profiles for the original CCZ potential (Ref. 16) at 25 and 26 K. The relative pressure P/P_{SVP} at which the calculations were performed are indicated by the labels in the graph.

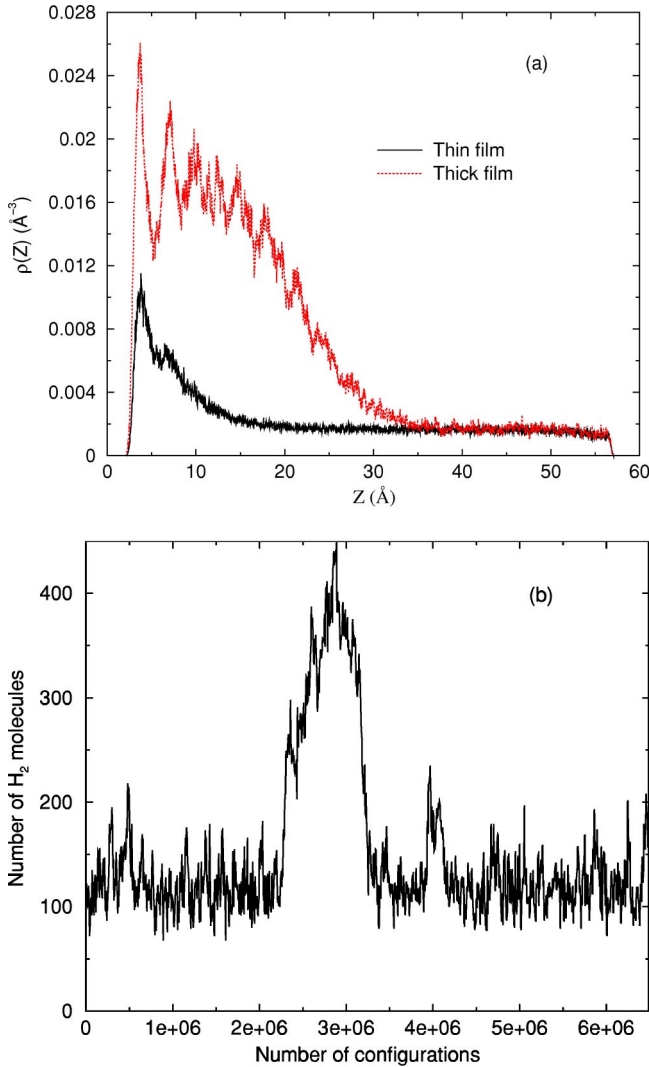


FIG. 3. (Color online) The local density profiles for the original CCZ potential (Ref. 16) at 26 K and $P/P_{SVP}=0.98$.

thin film of H_2 on Rb. The thin film density profile plotted in Fig. 3(a) was calculated from configurations containing from about 100 to 150 molecules. At about 2.5×10^6 configurations the system abruptly switches to a thick film, containing approximately 350 to 450 H_2 molecules. This thick film subsequently evaporates to a thin film at about 3.2×10^6 configurations. The thick film line in Fig. 3(a) was calculated from the data between about 2.5×10^6 and 3.2×10^6 configurations. The switching between thin and thick films is facilitated by the fact that the temperature of the transition is close to the bulk vapor-liquid critical temperature (~ 33 K) where the interfacial tension disappears.

The simulation value of $T_w = 25.5 \pm 0.5$ K is significantly higher than the experimentally measured value of $T_w = 19.10 \pm 0.06$ K.⁹ This discrepancy implies that the assumed $V(z)$ is too weakly attractive, which we address below. We have empirically adjusted $V(z)$ to bring the T_w prediction into agreement with experiment by making changes to C_{VDW} and V_0 . Some results are shown in Table I. We have also included in Table I the results for simulations using the empirical 9-3 potential, which is expected to be less accurate

TABLE I. Well depths (D), wetting temperatures, and prewetting critical points (T_{PWC}) for H_2 on Rb computed from the 9-3 potential (Ref. 10), the original CCZ potential (Ref. 16), and several variants obtained with altered parameters. The values of T_w in parentheses are determined from the simple model while the other values are from simulations (with uncertainty ± 0.5 K). The experimental values are $T_w = 19.1$ K and $T_{PWC} \sim 23$ K (Ref. 9).

Potential model	D (K)	T_w (K)	T_{PWC} (K)
9-3	44	29.5(22)	31
CCZ	41	25.5 (22.7)	30
$0.9 V_0$	45	22.5 (20.3)	28
$1.1 C_{VDW}$	49	18.5(19)	25.5
$0.9 V_0, 1.08 C_{VDW}$	53	17.5(18.6)	24.5

than the theoretically based CCZ potential. These results (and others, not tabulated) indicate the sensitivity of the wetting behavior to the potential parameters, especially the VDW coefficient. For example, for H_2 on Rb a 10% increase in C_{VDW} (i.e., to a value of $1.1 C_{VDW}$) leads to a 27% decrease in T_w , whereas a 10% decrease in V_0 (to $0.9 V_0$) gives a 12% decrease in T_w . Of the potentials we have examined, $1.1 C_{VDW}$ gives the best agreement with experiments.

Since one of the aims of this work is to test the simple model by producing the first conclusive comparison between experiment, theory, and simulations, we calculated the wetting temperature from Eq. (1) for various potentials. The simple model predicts a T_w of 22.7 K (Ref. 16) for the CCZ potential and a value of 22 K for the 9-3 potential. The simulations indicate that $T_w = 25.5 \pm 0.5$ K for the CCZ potential and 29.5 ± 0.5 K for the 9-3 potential. This finding was unexpected because the 9-3 potential has a substantially larger well depth than the CCZ potential (see Fig. 1), which would be expected to result in a *lower* T_w . This is reflected in the predictions from the simple model (see Table I). However, the simulations show that the broader potential well of the CCZ potential more than compensates for the smaller value of D compared with the 9-3 potential. This sensitivity to the shape of the potential does not appear to be adequately captured in the simple model. Moreover, we note that the prediction of T_w from the simple theory for both the CCZ and 9-3 potentials are not in good agreement with simulation values. Equation (1) underestimates T_w by 11% for the CCZ and 25% for the 9-3 potentials. In contrast, the value of T_w predicted from simple model for both of these potentials is in reasonably good agreement with the experimental value of 19.1 K from experiments.⁹ It is therefore apparent that the agreement with experiments is at least somewhat fortuitous.

In an attempt to bring the simple model into better agreement with the simulation data, we here include quantum effects in the solid-fluid potential for use in the simple model. The potentials used in Eq. (1) are classical and no corrections are made for the weakening of the potential that occurs at short distances due to the zero point energy of the adsorbate. However, this effect is properly included in the path integral simulations, since the effective solid-fluid interaction for a single molecule is given by an average of the potential between the solid and the ring polymer. The effective solid-

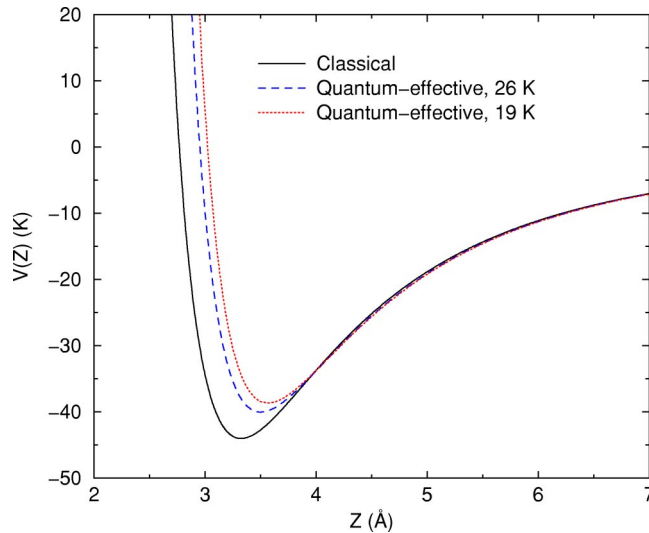


FIG. 4. (Color online) The empirical 9-3 (Ref. 10) classical and quantum-effective potentials for H_2 on Rb.

fluid potential, including quantum effects, is a function of temperature. The high temperature limit of the quantum-effective potential is identical to the classical solid-fluid potential. We have computed the quantum-effective potential for H_2 /Rb using the 9-3 potential at several different temperatures. The classical potential and quantum-effective potentials at two temperatures are plotted in Fig. 4. The quantum potentials were computed by inserting a single path (ring polymer) at fixed distances from the surface (z), choosing the orientation and conformation of the path randomly. Random path conformations were generated from a path integral simulation of the ideal gas at the corresponding temperature. An ensemble average over the orientations and conformations is performed at each value of z , giving the correct quantum-effective solid-fluid potential. As can be seen from Fig. 4, the well depth of the quantum-effective potential is considerably smaller than the classical potential at either 19 or 26 K. Calculation of T_w from Eq. (1) using the quantum-effective potential is an iterative process because of the temperature dependence of the potential. However, the calculation converges rapidly. We find that quantum effects on the solid-fluid potential only raise T_w by 2 K, or an increase of about 9% for the H_2 /Rb 9-3 system. Hence, the neglect of quantum effects on the solid-fluid potential gives a systematic error in T_w , but accounts for less than half of the discrepancy between the simple model and the simulations. The small magnitude of the correction is rather surprising given that quantum effects decrease the potential well depth by about 10% at these temperatures. We stress that use of the quantum-effective potential in the simple model is only useful for evaluating how T_w changes when quantum effects on the solid-fluid potential are included in the model. This correction is not justified in general since the model is surprisingly accurate as it stands.

Comparison of calculated and experimental T_w values implies that the CCZ potential is not sufficiently attractive to explain the H_2 /Rb data. We have made additional comparisons to test the generality of this conclusion. One compari-

son involves the adsorption of D_2 on Rb. This is a fairly stringent test of the new potential and its relation to the experiments, which were carried out in the same laboratory in which the H_2 /Rb data were taken. We have used the potential in best agreement with H_2 /Rb experimental data, i.e., $1.1C_{VDW}$, for these simulations. The result is that the simulation yields $T_w = 29 \pm 0.5$ K, in excellent agreement with the experimental value of 28.9 ± 0.3 K.⁹ This agreement improves our confidence in the new potential, which should be virtually identical for the two isotopes (differing only in very small effects of the 1% difference in the isotopes' polarizabilities). We have also studied H_2 wetting on a similar system, H_2 /Cs. The potential well-depth for H_2 /Cs was found by Chizmeshya *et al.*¹⁶ to be some 5% smaller than that for H_2 /Rb. The simple model predicts a $T_w \sim 23$ K, which is higher than the experimental value of 20.57 ± 0.05 K of Ross *et al.*¹¹ We have simulated this system with the $1.1C_{VDW}$ potential, assuming that the error in the *ab initio* potential is systematic. The resulting wetting temperature for this system is 19.5 ± 0.5 K which is slightly lower than the experimental result. The agreement for the three relevant systems that have been studied experimentally encourages our confidence in both the revised potential and the experiments. The comparison is particularly meaningful because the experiments were performed in different laboratories, using quite distinct methods of surface preparation.

We have computed T_w of H_2 on Au coated with Rb, a system not yet studied experimentally. The potential for this system is given by

$$V_{Rb/Au}(z) = V(z) - \frac{\delta c}{(z+d)^3}, \quad (3)$$

where $\delta c = 474$ meV \AA^3 is the difference of the C_{VDW} between Au and Rb, d is the film thickness of Rb, set to 15 \AA in this case, and $V(z)$ is given by Eq. (2) with the parameter for H_2 /Rb using $1.1C_{VDW}$. The potentials for H_2 interacting with a pure Rb surface and a 15 \AA film of Rb on Au are plotted in Fig. 5. Note that the potentials are nearly identical, with the Rb/Au potential being about 1 K deeper at the minimum. T_w for H_2 on a 15 \AA film of Rb on Au is 17.5 ± 0.5 K, about 1 K lower than the pure Rb case. The lowering of T_w has been observed for ^4He on Cs films of various thicknesses.⁵ At 20 K the relative prewetting transition pressure, P_w/P_{SVP} , is 0.93 for the Rb on Au substrate, while for the pure Rb substrate $P_w/P_{SVP} = 0.97$, a decrease of about 4%. The P_w/P_{SVP} at 21 K also differ by about 4%. These differences in T_w and P_w/P_{SVP} should be large enough to detect experimentally. We comment that estimates of P_w/P_{SVP} from the simulations are not very precise because of uncertainty in locating the transition chemical potential. Much more extensive simulations would be needed to map out the prewetting phase diagram with precision close to that of the experiments.⁹ Nevertheless, the predicted change in P_w/P_{SVP} from 0.97 to 0.94 at 20 K is larger than the uncertainty in the simulations. The simple theory predicts that the wetting temperature shifts in proportion to δc , with a resulting shift of 0.9 K for a Rb film thickness of 15 \AA .⁴⁶ This

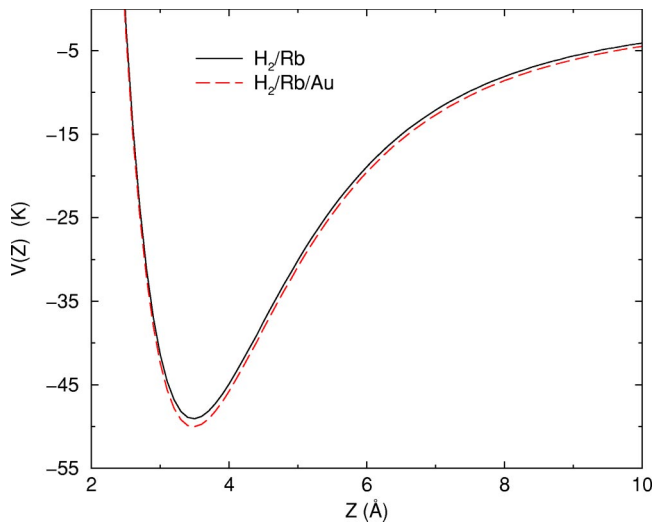


FIG. 5. (Color online) The CCZ (Ref. 16) for H_2 on Rb adjusted to fit experimental data [$1.1C_{VDW}$ (solid line)] and the corresponding potential for a 15 Å thick film of Rb on Au (dashed line).

prediction is consistent with the simulation result. The surprisingly large shift is indicative of the extreme sensitivity of the wetting transition behavior to the long range interaction, as implied by Eq. (1). It is possible to experimentally construct such a film of Rb on Au and to measure the wetting properties to test these predictions.⁵

We address briefly the intriguing question: why does the theoretical CCZ potential underestimate the gas-surface attraction by $\sim 10\%$? Possible explanations include surface roughness and substrate impurities in the experimentally produced materials, the contribution of the H_2 quadrupole interaction with its image (omitted from CCZ), uncertainty about the image plane's position, the form of the damping function, and the need for a more careful treatment of the electron gas, including hybridization with the adsorbate states.⁴⁷ When comparing experiments with theory in this field, it is important to recognize the potential effects of surface heterogeneity. In the case of the wetting experiments on alkali metals, the surfaces have not been characterized by either real space (STM) or diffractive techniques. However, experimentalists have reported effects on T_w of varying surface preparation method. One example involves one of the first reports of helium's wetting transition on Cs,⁴ which occurred far below the current estimated transition temperature (2 K). This lowering of the wetting temperature contrasts with a recent simulation result of an increase in wetting temperature,⁴⁸ but the latter involved an essentially classical gas on a specific model of surface imperfection. Thus, it appears to be the case

that the wetting temperature could either increase or decrease due to heterogeneity. Next, we consider the contributions of two independent quadrupole-related terms. The first is the permanent quadrupole moment's orientation-dependent interaction with its image, which has been evaluated elsewhere for similar problems.⁴⁹ The resulting energy is small: just 0.2 K (compared to a well depth of 41 K). The other term is the fluctuating quadrupole moment of the molecule interacting with its image in the metal. Using the theory of Jiang *et al.* to evaluate this quantity, we obtain an attractive energy of 2.0 K for an H_2 molecule at its equilibrium position on Rb.⁵⁰ This represents a 5% contribution to the well depth, too small to explain the discrepancy manifested in T_w . Thus, the adsorption potential remains an open problem.

Finally, we comment on the decade-long evolution of our understanding of this problem. A theoretical potential was proposed in 1993, from which the simple model predicted a wetting temperature ~ 22 K for H_2 /Rb, close to the experimental value of 19 K.¹⁰ This agreement was a fortuitous consequence, we now believe, of a systematic error inherent in the simple model (explained above) and a systematic error in the potential used at that time. These two errors shifted the prediction of T_w in opposite directions, so that their effects approximately canceled, resulting in nominal agreement with experiment. In that initial study, the uncertainty in the well depth of the potential was reported to be 40%. The more recent CCZ potential employs better justified methods and approximations than the 1993 study and has a smaller estimated uncertainty, $\sim 25\%$. However, the good agreement of 1993 between experiment and theory has been lost, leaving unanswered questions about the origin of the remaining discrepancy. The present study indicates how wetting transition data can be utilized to test and refine theoretical adsorption potentials. Complementary experimental investigations, such as gas-surface scattering measurements and a test of the predicted shift in T_w for the Rb/Au compound substrate, would provide additional assessments of predictions based on these new potentials.

Note added in proof: A recent study of HD scattering from Cs has been performed. The results of these experiments are semiquantitatively consistent with the CCZ potential, but are not able to discriminate errors in the potential on the order of 10%. See A. Siber, Ch. Boas, Ch. Wöll and M. W. Cole (unpublished).

ACKNOWLEDGMENTS

We thank Andrew Chizmeshya, Eugene Zaremba, Milen Kostov, and Giampaolo Mistura. We acknowledge NSF and NETL for support of this work.

*Electronic address: karlj@pitt.edu

¹J.W. Cahn, J. Chem. Phys. **66**, 3667 (1977).

²C. Ebner and W.F. Saam, Phys. Rev. Lett. **38**, 1486 (1977).

³J.E. Rutledge and P. Taborek, Phys. Rev. Lett. **69**, 937 (1992).

⁴K.S. Ketola, S. Wang, and R.B. Hallock, Phys. Rev. Lett. **68**, 201 (1992).

⁵P. Taborek and J.E. Rutledge, Phys. Rev. Lett. **71**, 263 (1997).

⁶A.F.G. Wyatt, J. Klier, and P. Stefanyi, Phys. Rev. Lett. **74**, 1151 (1995).

⁷D. Ross, P. Taborek, and J.E. Rutledge, Phys. Rev. Lett. **74**, 4483 (1995).

⁸D. Ross, J.A. Phillips, J.E. Rutledge, and P. Taborek, J. Low Temp. Phys. **106**, 81 (1997).

⁹G. Mistura, H.C. Lee, and M.H.W. Chan, J. Low Temp. Phys. **96**,

- 221 (1994).
- ¹⁰E. Cheng, G. Mistura, H.C. Lee, M.H.W. Chan, M.W. Cole, C. Carraro, W.F. Saam, and F. Toigo, *Phys. Rev. Lett.* **70**, 1854 (1993).
- ¹¹D. Ross, P. Taborek, and J.E. Rutledge, *Phys. Rev. B* **58**, R4274 (1998).
- ¹²G.B. Hess, M.J. Sabatini, and M.H.W. Chan, *Phys. Rev. Lett.* **78**, 1739 (1997).
- ¹³F. Hensel and M. Yao, *Eur. J. Solid State Inorg. Chem.* **34**, 861 (1997).
- ¹⁴V.F. Kozhevnikov, D.I. Arnold, S.P. Naurzakov, and M.E. Fisher, *Phys. Rev. Lett.* **78**, 1735 (1997).
- ¹⁵E. Cheng, M.W. Cole, W.F. Saam, and J. Treiner, *Phys. Rev. B* **48**, 18 214 (1993).
- ¹⁶A. Chizmeshya, M.W. Cole, and E. Zaremba, *J. Low Temp. Phys.* **110**, 677 (1998).
- ¹⁷F. Ancilotto, F. Faccin, and F. Toigo, *Phys. Rev. B* **62**, 17 035 (2000).
- ¹⁸F. Ancilotto and F. Toigo, *Phys. Rev. B* **60**, 9019 (1999).
- ¹⁹C. Ebner and W.F. Saam, *Phys. Rev. B* **35**, 1822 (1987).
- ²⁰F. Ancilotto, S. Curtarolo, F. Toigo, and M.W. Cole, *Phys. Rev. Lett.* **87**, 206103 (2001).
- ²¹E. Cheng, M.W. Cole, W.F. Saam, and J. Treiner, *Phys. Rev. Lett.* **67**, 1007 (1991).
- ²²S. Curtarolo, G. Stan, M.J. Bojan, M.W. Cole, and W.A. Steele, *Phys. Rev. E* **61**, 1670 (2000).
- ²³J.E. Finn and P.A. Monson, *Phys. Rev. A* **39**, 6402 (1989).
- ²⁴We note that Faccin *et al.* (Ref. 17) studied this transition with a finite T density functional method.
- ²⁵M.J. Bojan, M.W. Cole, J.K. Johnson, W.A. Steele, and Q. Wang, *J. Low Temp. Phys.* **110**, 653 (1998).
- ²⁶M. Boninsegni and M.W. Cole, *J. Low Temp. Phys.* **110**, 685 (1998).
- ²⁷M. Wagner and D.M. Ceperley, *J. Low Temp. Phys.* **94**, 185 (1994).
- ²⁸R.P. Feynman, *Rev. Mod. Phys.* **20**, 367 (1948).
- ²⁹Q.Y. Wang and J.K. Johnson, *Fluid Phase Equilib.* **132**, 93 (1997).
- ³⁰D.M. Ceperley, *Rev. Mod. Phys.* **67**, 279 (1995).
- ³¹Q.Y. Wang, J.K. Johnson, and J.Q. Broughton, *J. Chem. Phys.* **107**, 5108 (1997).
- ³²S. Duane, A.D. Kennedy, B.J. Pendleton, and D. Roweth, *Phys. Lett. B* **195**, 216 (1987).
- ³³M.E. Tuckerman, B.J. Berne, G.J. Martyna, and M.L. Klein, *J. Chem. Phys.* **99**, 2796 (1993).
- ³⁴M.E. Tuckerman, B.J. Berne, and G.J. Martyna, *J. Chem. Phys.* **97**, 1990 (1992).
- ³⁵M. P. Allen and D. J. Tildesley, *Computer Simulation of Liquids* (Clarendon, Oxford, 1987).
- ³⁶I.F. Silvera and V.V. Goldman, *J. Chem. Phys.* **69**, 4209 (1978).
- ³⁷W. Shi and J. K. Johnson (unpublished).
- ³⁸X. C. Zhao, J. K. Johnson, and C. E. Rasmussen (unpublished).
- ³⁹A.M. Ferrenberg and R.H. Swendsen, *Phys. Rev. Lett.* **61**, 2635 (1988).
- ⁴⁰A.M. Ferrenberg and R.H. Swendsen, *Phys. Rev. Lett.* **63**, 1195 (1989).
- ⁴¹E. Zaremba and W. Kohn, *Phys. Rev. B* **15**, 1769 (1977).
- ⁴²M.J. Bojan, G. Stan, S. Curtarolo, W.A. Steele, and M.W. Cole, *Phys. Rev. E* **59**, 864 (1999).
- ⁴³S. Sokołowski and J. Fischer, *Phys. Rev. A* **41**, 6866 (1990).
- ⁴⁴Y. Fan and P.A. Monson, *J. Chem. Phys.* **99**, 6897 (1993).
- ⁴⁵Y. Fan, J.E. Finn, and P.A. Monson, *J. Chem. Phys.* **99**, 8238 (1993).
- ⁴⁶E. Cheng, M.W. Cole, W.F. Saam, and J. Treiner, *J. Low Temp. Phys.* **89**, 739 (1992).
- ⁴⁷J.F. Annett and R. Haydock, *Phys. Rev. B* **34**, 6860 (1986).
- ⁴⁸S. Curtarolo, G. Stan, M.W. Cole, M.J. Bojan, and W.A. Steele, *Phys. Rev. E* **59**, 4402 (1999).
- ⁴⁹L.W. Bruch, *J. Chem. Phys.* **79**, 3148 (1983).
- ⁵⁰X.P. Jiang, F. Toigo, and M.W. Cole, *Chem. Phys. Lett.* **101**, 159 (1983).